

Crossover in the electron-phonon heat exchange in layered nanostructures

Dragos-Victor Anghel,¹ Claudiu Caraiani,² and Yuri M. Galperin³

¹*Horia Hulubei National Institute for R&D in Physics and Nuclear Engineering, Măgurele, Romania*

²*University of Bucharest, Faculty of Physics, Măgurele, Romania*

³*Department of Physics, Unversity of Oslo, PO Box 1048 Blindern, 0316 Oslo, Norway and A. F. Ioffe Physico-Technical Institute of Russian Academy of Sciences, 194021 St. Petersburg, Russia*

(Dated: October 3, 2018)

We study theoretically the effect of the effective dimensionality of the phonon gas distribution on the heat exchange between electrons and phonons in layered nanostructures. If we denote the electrons temperature by T_e and the phonons temperature by T_{ph} , then the total heat power P is proportional—in general—to $T_e^x - T_{ph}^x$, the exponent x being dependent on the effective dimensionality of the phonon gas distribution. If we vary the temperature in a wide enough range, the effective dimensionality of the phonon gas distribution changes going through a crossover around some temperature, T_C . These changes are reflected by a change in x . On one hand, in a temperature range well below a crossover temperature T_C only the lowest branches of the phonon modes are excited. They form a (quasi) two-dimensional gas, with $x = 3.5$. On the other hand, well above T_C , the phonon gas distribution is quasi three-dimensional and one would expect to recover the three dimensional results, with $x = 5$. But this is not the case in our layered structure. The exponent x has a complicated, non-monotonous dependence on temperature forming a “plateau region” just after the crossover temperature range, with x between 4.5 and 5. After the plateau region, x decreases, reaching values between 3.5 and 4 at the highest temperature used in our numerical calculations, which is more than 40 times higher than T_C .

PACS numbers: 73.50.Lw, 85.80.Fi, 85.25.-j, 73.23.-b

I. INTRODUCTION

Continuous efforts in miniaturizing devices require better understanding of their quantum behaviors at nanoscale lengths and sub-Kelvin temperatures. Such devices are, e.g., microrefrigerators, microbolometers, and microcalorimeters.¹ The microrefrigerators have been proven to be able to reduce the temperature of the electron gas of a normal metal island down to 30 mK, starting from a bath temperature of 150 mK.² Such experimental achievement allows the use of these devices in refrigerating microbolometers, microcalorimeters, qubits, etc.

The devices are usually layered structures consisting of thin metal films (for example, Cu, Al, etc.) deposited on free standing dielectric membranes, typically made of sil-

icon nitride (SiN). The membrane is itself supported by a bulk substrate, which may be considered the thermostat for the whole device. A central issue in the understanding of how the devices function or how they respond to the absorption of electromagnetic radiation is the interaction and the heat exchange between the electron system and the phonon system in the normal metal films. Our study is based on the model presented in Refs. 3 and 4, in which a Cu layer of thickness d is deposited on a SiN membrane of thickness $L - d$, such that the total thickness of the system is L . The temperature range in which the microcalorimeters operate is several hundreds of mK.^{1,2} For typical values of L , which is of the order of 100 nm, and the sound velocities of the SiN, the dominant phonon wavelength of a three-dimensional (3D) phonon

gas model is comparable to L at temperatures of the order of 100 mK. As the temperature decreases, the 3D dominant phonon wavelength may become much bigger than L and excitations of phonon modes perpendicular to the membrane surfaces become very unlikely. In such a case, we can consider the phonon gas as being two-dimensional (2D). In the other extreme, at high enough temperatures, the dominant phonon wavelength may become much smaller than L and the phonon gas is practically 3D.^{5–8}

At temperatures of the order of 1 K, due to the depopulation of the phonon modes and the degeneracy of the electrons system, the two subsystems of a normal metal—the electrons and the phonons—become almost isolated from each other (see, e.g., the discussion in Sec. II of Ref. 1). For this reason, they can “equilibrate” independently, that is, they may reach equilibrium distributions over the quasiparticle states at some effective temperatures that we shall denote by T_e (for electrons) and T_{ph} (for phonons).⁹ Using the effective temperatures, the heat exchange P between the electrons and the phonons may be written in most cases as^{10–13}

$$P = V\Sigma(T_e^x - T_{ph}^x), \quad (1a)$$

where V is the volume and Σ is a constant of material. The exponent x varies, depending on the model and the dimensionalities of the electrons and the phonon gases. For 3D models, $x = 5$,¹⁰ for quasi-2D ones, $x = 4$,¹¹ whereas for a 1D phonon gas coupled to a 3D electrons system, $x = 3$.¹³ Apparently, this leads to the conjecture

$$x = 2 + s \quad (1b)$$

where s is the dimensionality of the phonon gas. Apart from Eq. (1b), it was observed that s may take also fractional values: if the phonon gas is 2D and the electron gas distribution is a superposition of 2D conduction bands, then $x = 3.5$.^{3,4}

The exponent x depends on the effective dimensionality of the phonon gas, but the latter may change with

temperature, as we discussed above.^{5–8} Therefore, in a temperature range where the dimensionality of the phonon gas changes, the exponent x may also change, showing a crossover between the values corresponding to different dimensionalities. This issue, which, to the best of our knowledge, has not been investigated will be explored here, as a continuation of previous studies.^{3,4}

The paper is organized as follows. In the next section we present the theory, with the system’s specifications, then, we present the results, and finally, we draw the conclusions. In the following, we try to preserve the notations from Refs. 3 and 4 as much as possible.

II. THEORY

As in Refs. 3 and 4, we consider a metallic film (for example, Cu) deposited on a free-standing dielectric membrane (for example silicon nitride) and perfectly glued to it.^{14,15} For the mathematical description, we choose a Cartesian system of coordinates, such that all the surfaces of the membrane and of the film are parallel to the (xy) plane. In the z direction, the membrane extends in the interval $[-L/2, L/2 - d]$, whereas the metal occupies the interval $[L/2 - d, L/2]$. In the x and y directions, the system is considered to be very large (in comparison with the wavelengths of the quasiparticles involved) and has the area A ; we assume that $L \ll \sqrt{A}$.

A. Description of the electrons

The metal contains free electrons, which interact with the phonons that propagate in the whole system. The electrons’ wave functions propagate in the (xy) plane and are confined along the z direction. We denote the electron’s wavevector by $\mathbf{k} \equiv (\mathbf{k}_{\parallel}, k_z)$, where \mathbf{k}_{\parallel} and k_z are the components of \mathbf{k} perpendicular and parallel to the z axis, respectively. For \mathbf{k}_{\parallel} , we impose periodic boundary conditions in the (xy) plane, whereas for k_z we impose Dirichlet boundary conditions at $z = L/2 - d$ and

$z = L/2$. This leads to a density of (allowed quantum) states (DOS) in the \mathbf{k}_{\parallel} variable equal to $A/(2\pi)^2$ and to the quantization condition $k_z \equiv n\pi/d$, where n is an integer. Then, the electron's wavefunction is of the form

$$\psi_{\mathbf{k}_{\parallel},n}(\mathbf{r},t) \equiv \psi_{\mathbf{k}_{\parallel},k_z}(\mathbf{r},t) = \phi_{k_z}(z)e^{i(\mathbf{k}_{\parallel}\mathbf{r}_{\parallel} - \epsilon_{\mathbf{k}_{\parallel},n}t/\hbar)}/\sqrt{A},$$

where $\phi_{k_z}(z) = \sqrt{\frac{2}{d}} \sin[(z + d - \frac{L}{2})k_z]$ and the electron's energy is

$$\epsilon_{\mathbf{k}} = \frac{\hbar^2 k^2}{2m_e} = \frac{\hbar^2 k_{\parallel}^2}{2m_e} + \frac{\hbar^2 k_z^2}{2m_e} \equiv \epsilon_{k_{\parallel},k_z},$$

where m_e is the free electron mass. In these notations, the electron annihilation and creation field operators are

$$\Psi(\mathbf{r},t) = \sum_{\mathbf{k}_{\parallel},k_z} \psi_{\mathbf{k}_{\parallel},k_z}(\mathbf{r},t)c_{\mathbf{k}_{\parallel},k_z} \quad (2a)$$

$$\Psi^{\dagger}(\mathbf{r},t) = \sum_{\mathbf{k}_{\parallel},k_z} \psi_{\mathbf{k}_{\parallel},k_z}^*(\mathbf{r},t)c_{\mathbf{k}_{\parallel},k_z}^{\dagger}, \quad (2b)$$

respectively, where $c_{\mathbf{k}_{\parallel},k_z}$ and $c_{\mathbf{k}_{\parallel},k_z}^{\dagger}$ are the electron annihilation and creation operators on the state $\psi_{\mathbf{k}_{\parallel},k_z}$.

Since $\sqrt{A} \gg L > d$, $\mathbf{k}_{\parallel} \equiv (k_x, k_y)$ has a quasi-continuous spectrum, whereas k_z will be considered discreet. States of constant k_z (or n) and any value of k_{\parallel} form the 2D *conduction bands*. We denote by n_F the number of occupied 2D bands at $T_e = 0$ K,

$$n_F \equiv \left\lfloor \frac{\sqrt{2m_e E_F}}{\pi\hbar} d \right\rfloor, \quad (3)$$

where $\lfloor x \rfloor$ is the biggest integer smaller or equal to x and E_F is the Fermi energy. If the normal metal is Cu, $E_F \approx 7$ eV and for $d = 10$ nm, $n_F = 43$, whereas for $d = 20$ nm, $n_F = 86$.

B. Description of the phonons

The phonons are quanta of elastic vibrations of the system. They propagate in the (xy) plane and are stationary waves along z . At the surfaces of the system, at $z = \pm L/2$, the phonons satisfy free boundary conditions. To simplify the calculation of the phonon modes,^{3,4} we consider that the metal and the dielectric membrane

have identical mechanical properties, namely they have the same mass density and identical elastic properties. Although this seems to be a crude simplification, it gives us a method to study the characteristics of the electron-phonon interaction in general.

The phonon modes are eigenstates of the elastic dynamic equations and are grouped in three polarizations: horizontal shear (h), symmetric (s) and antisymmetric (a) modes¹⁶. While the h modes are pure transversal (t) vibrations, the s and a modes are superpositions of transversal and longitudinal (l) vibrations¹⁶—in a longitudinal vibration, the displacement field is in the propagation direction, whereas in a transversal vibration the displacement field and the propagation direction are perpendicular to each other.

An h mode is characterized by a single wavevector, of components $(\mathbf{q}_{\parallel}, q_t)$, perpendicular and parallel to the z axis, respectively. The component \mathbf{q}_{\parallel} satisfy periodic boundary conditions in the (xy) plane and $q_t \equiv \nu\pi/L$, where $\nu = 0, 1, \dots$. States of constant ν and variable \mathbf{q}_{\parallel} define 2D *phonon branches*.

An s mode—and, similarly, an a mode—is characterized by two wavevectors, corresponding to the l and t vibrations. The wavevector corresponding to the longitudinal vibration has the components \mathbf{q}_{\parallel} and q_l , whereas the wavevector of the transversal vibration has the components \mathbf{q}_{\parallel} and q_t . The component \mathbf{q}_{\parallel} , perpendicular to the z axis, is the same for both, l and t vibrations, whereas the components q_l and q_t , parallel to the z axis, are, in general, different. As in the case of electrons, \mathbf{q}_{\parallel} satisfies periodic boundary conditions on the area A and has a DOS of $A/(2\pi)^2$. The free boundary conditions imposed at $z = \pm L/2$ lead to the equation^{4,16}

$$\frac{-4q_{\parallel}^2 q_l \xi q_t \xi}{(q_{\parallel}^2 - q_t^2 \xi)^2} = \left[\frac{\tan(q_t \xi L/2)}{\tan(q_l \xi L/2)} \right]^{\pm 1}, \quad (4a)$$

for the components q_l and q_t , where $q_{\parallel} \equiv |\mathbf{q}_{\parallel}|$. The exponents $+1$ and -1 on the right hand side (rhs) of Eq. (4a) correspond to the polarizations s and a , respectively¹⁶, whereas $\xi \equiv (\alpha, \nu)$ is a doublet, containing the polariza-

tion $\alpha = s, a$ and the branch number $\nu = 0, 1, 2, \dots$ (as in the case of the h polarization), as we shall specify below. If we denote by c_l and c_t the longitudinal sound velocity and the transversal sound velocity, respectively, then the angular frequency, common to both, longitudinal and transversal vibrations, is given by

$$\omega_{q_{\parallel}\xi} = c_l \sqrt{q_{t,\xi}^2 + q_{\parallel}^2} = c_t \sqrt{q_{t,\xi}^2 + q_{\parallel}^2}. \quad (4b)$$

The system (4) has a countable, infinite number of solutions, for each α and q_{\parallel} . These solutions are denoted by ν and form the branches, when plotted as functions of q_{\parallel} . In general, $q_{t\alpha\nu}$ and $q_{l\alpha\nu}$ may take both, (positive) real and imaginary values, as explained for example in¹⁶ (see also¹⁷), whereas q_{\parallel} takes only real positive values, by definition. If ρ is the mass density of the system (considered homogeneous in the whole volume), then the sound velocities may be expressed in terms of the Lamé

coefficients λ and μ ¹⁶,

$$c_t^2 = \frac{\mu}{\rho}, \quad c_l^2 = \frac{\lambda + 2\mu}{\rho}, \quad (5)$$

and we define $J \equiv c_t^2/c_l^2$.

We define the elastic modes by $\mathbf{w}_{\mathbf{q}_{\parallel}\xi}(z) e^{i(\mathbf{q}_{\parallel}\mathbf{r}_{\parallel} - \omega_{\mathbf{q}_{\parallel}\xi}t)}/\sqrt{A}$, where the functions $\mathbf{w}_{\mathbf{q}_{\parallel}\xi}(z)$ are normalized such that $\int_{-L/2}^{L/2} \mathbf{w}_{\mathbf{q}_{\parallel}\xi}(z)^\dagger \mathbf{w}_{\mathbf{q}_{\parallel}\xi'}(z) dz = \delta_{\xi,\xi'}$ and have the following analytical expressions,^{3,4}

$$w_{\mathbf{q}_{\parallel},s,\nu,x} = N_s i q_t \left[2q_{\parallel}^2 \cos\left(\frac{q_t L}{2}\right) \cos(q_l z) + (q_t^2 - q_{\parallel}^2) \times \cos\left(\frac{q_l L}{2}\right) \cos(z q_t) \right], \quad (6a)$$

$$w_{\mathbf{q}_{\parallel},s,\nu,z} = N_s q_{\parallel} \left[-2q_t q_l \cos\left(\frac{q_t L}{2}\right) \sin(q_l z) + (q_t^2 - q_{\parallel}^2) \times \cos\left(\frac{q_l L}{2}\right) \sin(z q_t) \right], \quad (6b)$$

$$w_{\mathbf{q}_{\parallel},a,\nu,x} = N_a i q_t \left[2q_{\parallel}^2 \sin\left(\frac{q_t L}{2}\right) \sin(q_l z) + (q_t^2 - q_{\parallel}^2) \times \sin\left(\frac{q_l L}{2}\right) \sin(z q_t) \right], \quad (6c)$$

$$w_{\mathbf{q}_{\parallel},a,\nu,z} = N_a q_{\parallel} \left[2q_t q_l \sin\left(\frac{q_t L}{2}\right) \cos(q_l z) - (q_t^2 - q_{\parallel}^2) \times \sin\left(\frac{q_l L}{2}\right) \cos(z q_t) \right], \quad (6d)$$

with the normalization constants

$$\frac{1}{N_s^2} = A \left\{ 4q_t^2 q_{\parallel}^2 \cos^2(q_t L/2) \left[(p_l^2 + q_{\parallel}^2) \frac{\sinh(p_l L)}{2p_l} - (p_l^2 - q_{\parallel}^2) \frac{L}{2} \right] + (q_t^2 - q_{\parallel}^2)^2 \cosh^2(p_l L/2) \left[(q_t^2 + q_{\parallel}^2) \frac{L}{2} + (q_t^2 - q_{\parallel}^2) \frac{\sin(q_t L)}{2q_t} \right] - 4q_{\parallel}^2 q_t (q_t^2 - q_{\parallel}^2) \cosh^2\left(\frac{p_l L}{2}\right) \sin(q_t L) \right\}, \quad (7a)$$

$$\frac{1}{N_a^2} = A \left\{ 4p_t^2 q_{\parallel}^2 \sinh^2(p_t L/2) \left[(p_l^2 + q_{\parallel}^2) \frac{\sin(p_l L)}{2p_l} + (p_l^2 - q_{\parallel}^2) \frac{L}{2} \right] + (p_t^2 - q_{\parallel}^2)^2 \sinh^2(p_t L/2) \left[(p_t^2 + q_{\parallel}^2) \frac{\sinh(p_t L)}{2} - (p_t^2 - q_{\parallel}^2) \frac{L}{2p_t} \right] - 4q_{\parallel}^2 p_t (p_t^2 + q_{\parallel}^2) \sinh^2\left(\frac{p_t L}{2}\right) \sinh(p_t L) \right\}. \quad (7b)$$

Then the displacement field operator is

$$\mathbf{u}(\mathbf{r}, t) = \sum_{\xi, \mathbf{q}_{\parallel}} \sqrt{\frac{\hbar}{2\rho\omega_{\mathbf{q}_{\parallel}\xi}}} e^{i(\mathbf{q}_{\parallel}\mathbf{r}_{\parallel} - i\omega_{\mathbf{q}_{\parallel}\xi}t)} \times \left[a_{\mathbf{q}_{\parallel}\xi} \mathbf{w}_{\mathbf{q}_{\parallel}\xi}(z) + a_{-\mathbf{q}_{\parallel}\xi}^\dagger \mathbf{w}_{\mathbf{q}_{\parallel}\xi}^*(z) \right], \quad (8)$$

where $a_{\mathbf{q}_{\parallel}\xi}^\dagger$ and $a_{\mathbf{q}_{\parallel}\xi}$ are the phonon creation and annihilation operators.

In the following we shall write q_t instead of $q_{t,\xi}$ and q_l instead of $q_{l,\xi}$, when this does not lead to confusions.

The electron-phonon interaction is calculated in the deformation potential model, employing the interaction Hamiltonian,¹⁸

$$H_{\text{def}} = \frac{2}{3} E_F \int_{V_{el}=A \times d} d^3\mathbf{r} \Psi^\dagger(\mathbf{r}) \Psi(\mathbf{r}) \nabla \cdot \mathbf{u}(\mathbf{r}). \quad (9)$$

Starting from Eq. (9) and applying the Fermi golden rule $\Gamma_{i \rightarrow f}(2\pi/\hbar)|\langle f|H_{\text{def}}|i\rangle|^2\delta(E_f - E_i)$ to calculate the transition rates Γ between the initial state $|i\rangle$, of energy E_i , and the final state $|f\rangle$, of energy E_f , the heat power was calculated in Refs. 3 and 4 to be

$$P \equiv P^{(0)}(T_e) - P^{(1)}(T_e, T_{ph}), \quad (10a)$$

where

$$P^{(0)}(T_e) \equiv P_s^{(0)}(T_e) + P_a^{(0)}(T_e), \quad (10b)$$

$$P^{(1)}(T_e, T_{ph}) \equiv P_s^{(1)}(T_e, T_{ph}) + P_a^{(1)}(T_e, T_{ph}), \quad (10c)$$

$$P_\alpha^{(0)}(T_e) \equiv \frac{4\pi}{\hbar} \sum_{\mathbf{k}_\parallel \mathbf{k}'_\parallel, n, n'}^{\mathbf{q}_\parallel, \nu} \hbar\omega_{\mathbf{q}_\parallel, \alpha, \nu} |g_{\alpha, \nu, \mathbf{q}_\parallel}^{n', n}|^2 \times [f(\beta_e \epsilon_{\mathbf{k}_\parallel - \mathbf{q}_\parallel, n'}) - f(\beta_e \epsilon_{\mathbf{k}_\parallel, n})] n(\beta_e \epsilon_{\mathbf{q}_\parallel, \nu}), \quad (10d)$$

$$P_\alpha^{(1)}(T_e, T_{ph}) \equiv \frac{4\pi}{\hbar} \sum_{\mathbf{k}_\parallel \mathbf{k}'_\parallel, n, n'}^{\mathbf{q}_\parallel, \nu} \hbar\omega_{\mathbf{q}_\parallel, \alpha, \nu} |g_{\alpha, \nu, \mathbf{q}_\parallel}^{n', n}|^2 \times [f(\beta_e \epsilon_{\mathbf{k}_\parallel - \mathbf{q}_\parallel, n'}) - f(\beta_e \epsilon_{\mathbf{k}_\parallel, n})] n(\beta_{ph} \epsilon_{\mathbf{q}_\parallel, \nu}), \quad (10e)$$

whereas $\alpha = s$ or a .^{3,4} We also used the notation

$$g_{\xi, \mathbf{q}_\parallel}^{n', n} = \frac{2}{3} E_F N_{\xi, \mathbf{q}_\parallel} \sqrt{\frac{\hbar}{2\rho\omega_{\mathbf{q}_\parallel, \xi}}} \int_{L/2-d}^{L/2} \phi_{n'}^*(z) \phi_n(z) \times \left[i\mathbf{q}_\parallel \cdot \mathbf{w}_{\mathbf{q}_\parallel, \xi}(z) + \frac{d\omega_{\mathbf{q}_\parallel, \xi}(z)}{dz} \right] dz, \quad (11)$$

where the normalization constants $N_{\xi, \mathbf{q}_\parallel}$ are given in Eqs. (7).

With the power defined by Eqs. (10), the exponents of the temperature dependence, as defined in (1a), are calculated as

$$x_{T_{ph}} \equiv -\frac{\partial \ln(P)}{\partial \ln(T_{ph})} \quad \text{and} \quad x_{T_e} \equiv \frac{\partial \ln(P)}{\partial \ln(T_e)}. \quad (12a)$$

Although in Eq. (1a) we have only one exponent x , in Eq. (12) we introduce both, $x_{T_{ph}}$ and x_{T_e} , to check the consistency of the description.

If $P^{(1)}$ does not depend on T_e (as we shall see further) and since $P^{(0)}$ does not depend on T_{ph} , then we may write Eqs. (12a) as

$$x_{T_{ph}} = -\frac{\partial \ln(P^{(1)})}{\partial \ln(T_{ph})} \quad \text{and} \quad x_{T_e} = \frac{\partial \ln(P^{(0)})}{\partial \ln(T_e)}. \quad (12b)$$

III. RESULTS

For concreteness, we consider systems of total thickness $L = 100$ nm, of which, the thickness of the metallic film is around 10 nm. The elastic properties of the entire system correspond to the silicon nitride, which is a common material for the construction of the supporting membrane of nano-detectors.¹ For this material, the density is $\rho = 3290$ kg/m³, whereas the longitudinal and transversal sound velocities are $c_l = 10300$ m/s and $c_t = 6200$ m/s, respectively. The crossover temperature is defined as $T_C = c_t \hbar / (2k_B L) \approx 237$ mK,⁷ and in the low temperature limit ($T \ll T_C$) only the lowest s and a phonon branches contribute to the electron-phonon interaction, since the upper branches are depopulated.^{3,4} As the temperature is increasing, the phonon gas changes dimensionality in a temperature interval around T_C and upper s and a branches gradually start to be populated and play a role in the interaction.

In the electron system, all the bands, from 1 to n_F , are populated at any temperature and contribute – with the electrons close to the Fermi energy – to the electron-phonon interaction. To estimate the difference between the energies of electrons of the same k_\parallel , but belonging to different 2D conduction bands, for a metallic layer of thickness $d = 10$ nm, we calculate $(\epsilon_{\mathbf{k}_\parallel=0, n=2} - \epsilon_{\mathbf{k}_\parallel=0, n=1})/k_B \approx 131$ K and $(\epsilon_{\mathbf{k}_\parallel=0, n=44} - \epsilon_{\mathbf{k}_\parallel=0, n=43})/k_B \approx 3796$ K. We observe that this difference is very large in comparison with the energy of the thermal phonons, so scattering of electrons between different conduction bands are very rare and therefore they do not contribute to the electron-phonon heat exchange in a temperature range below 10 K (see also^{3,4}).

In Fig. 1 (a) we plot $P^{(0)}$ vs T_e and d . We observe the formation of the narrow crests, separated by valleys, as in Refs. 3 and 4. Both, T_e and $P^{(0)}/V_{el}$ are plotted in logarithmic scale and we observe a change of the slope of $\ln P^{(0)}$ vs $\ln T_e$, indicating a dimensionality crossover of the phonon gas distribution. Apparently, the slope is

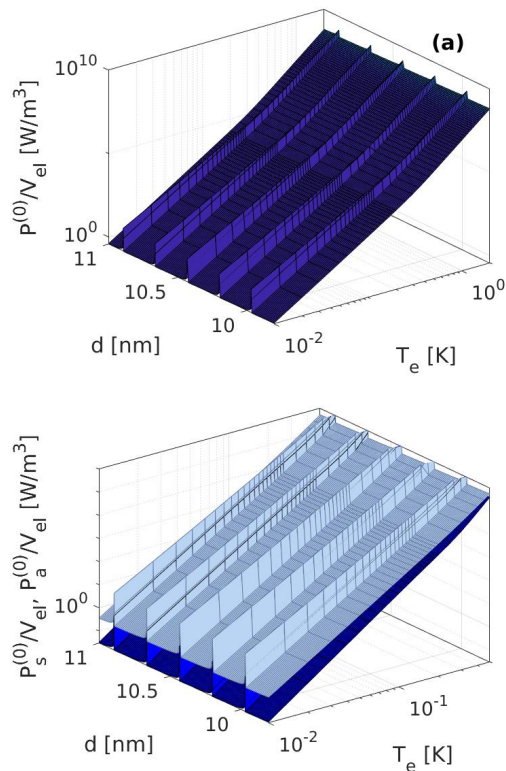


FIG. 1. (a) The heat power $P^{(0)}$, as a function of T_e and the thickness d of the metallic layer. In (b) we show separately (and on a smaller T_e range, for clarity) the contribution of the symmetric modes $P_s^{(0)}$ (dark blue, below) and of the antisymmetric modes $P_a^{(0)}$ (light blue, above). In the low temperature limit, $P_s^{(0)} < P_a^{(0)}$ for any d .

increasing with temperature, but more details are seen in Fig. 2, where we show a larger temperature interval. In Fig. 1 (b) we plot separately the contribution of the symmetric phonon modes $P_s^{(0)}$ (lower values in the low temperature limit) and of the antisymmetric phonon modes $P_a^{(0)}$ (higher values in the low temperature limit).

Similarly, we calculated $P_s^{(1)}(T_e, T_{ph})$, $P_a^{(1)}(T_e, T_{ph})$, and $P^{(1)}(T_e, T_{ph}) \equiv P_s^{(1)}(T_e, T_{ph}) + P_a^{(1)}(T_e, T_{ph})$. In the valleys (between crests) and in the temperature range investigated by us, both, $P_s^{(1)}$ and $P_a^{(1)}$ are independent of T_e , whereas their dependence on T_{ph} is the same with that of $P_s^{(0)}$ and $P_a^{(0)}$ on T_e , within the numerical accuracy. Introducing a notation, T_x , for both, T_e and T_{ph} ,

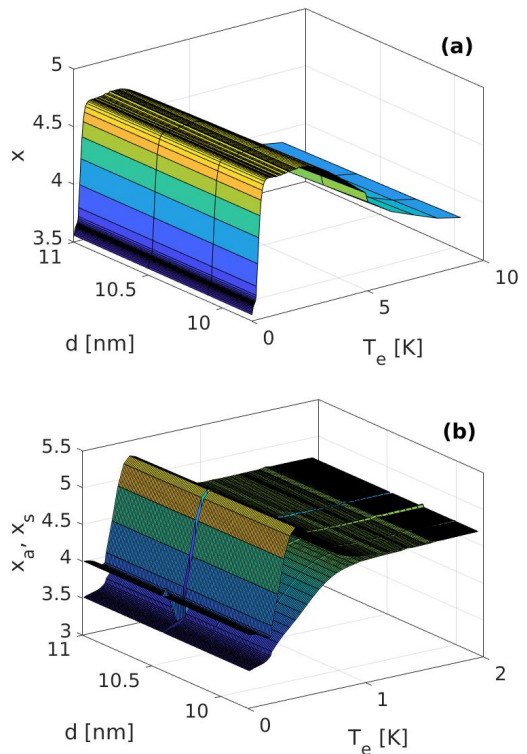


FIG. 2. The exponent of the temperature dependence.

and a constant value T_{e0} , we may write, formally,

$$P_s^{(1)}(T_{e0}, T_x) = P_s^{(0)}(T_x) \quad \text{and} \quad P_a^{(1)}(T_{e0}, T_x) = P_a^{(0)}(T_x). \quad (13)$$

For this reason we do not plot also $P_s^{(1)}$, $P_a^{(1)}$ or $P^{(1)}(T_e, T_{ph})$ vs T_{ph} and d . Numerically, these plot would be identical with the plots in Fig. 1.

In Fig. 2(a) we plot the exponent of the temperature dependence of $P^{(0)}$, denoted simply as x —since from Eqs. (12) and (13) we now know that $x_{T_e} = x_{T_{ph}}$. At low T_e , $x = 3.5$ (see^{3,4}), then increases with temperature to a value between 4.5 and 5 (not to 5, as expected from¹⁰) and varies little in an interval $T_e \in [0.5 \text{ K}, 3.5 \text{ K}]$, forming the “plateau region.” Quite surprisingly, at temperatures above above the plateau ($T_e > 3.5 \text{ K}$) the exponent decreases again, reaching a value between 3.5 and 4, at $T_e = 10 \text{ K}$. This is surprising because $T_e = 10 \text{ K}$ is more than 1 order of magnitude above the crossover temperature T_C and we would expect that at such temperatures the value of x should correspond to a 3D phonon gas

$x = 5$,¹⁰ see Eq. (1b) and the discussion around it.

In Fig. 2(b) we show the exponents of the temperature dependence of both, $P_s^{(0)}$ and $P_a^{(0)}$,

$$\begin{aligned} x_s &\equiv \frac{\partial \ln(P_s^{(0)})}{\partial \ln(T_e)} = \frac{\partial \ln(P_s^{(1)})}{\partial \ln(T_{ph})}, \\ x_a &\equiv \frac{\partial \ln(P_a^{(0)})}{\partial \ln(T_e)} = \frac{\partial \ln(P_a^{(1)})}{\partial \ln(T_{ph})} \end{aligned} \quad (14)$$

in a temperature range between 0 and 2 K. This is a higher resolution image, where we can notice also the crests. Nevertheless, in the crests regions the numerical errors are big, due to the high gradients and we shall not take them into account in our discussion. In the low temperature limit, $x_s = 4$ and $x_a = 3.5$. We notice that x_a increases from the low temperature value to a value between 4.5 and 5 in the plateau region (see above), after passing a crossover region around T_C .

The variation of x_s is more complicated, as it can be seen in Fig. 2(b). In the low temperature limit, $x_s = 4$ and then oscillates in the crossover region, until it reaches the plateau, where it becomes practically equal to x_a . Notice that in the crossover region x_s increases above 5 (which is supposed to be the 3D value). At the plateau and after it, x_s , x_a , and x become gradually (as temperature increases) numerically indistinguishable. For this reason, there was no point in plotting separately x_s and x_a at temperatures above 2 K.

IV. CONCLUSIONS

We studied the effect of the dimensionality of the phonon gas distribution on the heat exchange between electrons and phonons in a layered structure, consisting of a metallic layer (in our case, Cu) of thickness around 10 nm deposited on an insulating free standing membrane. The total thickness of the system (metal plus supporting membrane) is $L = 100$ nm. From a mechanical point of view (elastic properties and mass density) the system is considered homogeneous—the elastic waves propagate through a homogeneous material, making no

difference between the metal and the dielectric membrane. The longitudinal sound velocity, the transversal sound velocity, and the density of the system are considered to be those of the silicon nitride. With these parameters, the crossover temperature around which the phonon gas distribution changes from two-dimensional (at lower temperatures) to three dimensional (at higher temperatures) is $T_C \approx 237$ mK.⁷

We denoted the electron temperature by T_e and the phonon temperature by T_{ph} . The heat power P is expected to be described by the ansatz (1). It was already noticed that the ansatz does not apply to our type of layered system and in the low temperature limit, the exponent corresponding to the 2D phonon gas distribution is $x = 3.5$, not 4.^{3,4} We recovered here the results of Refs. 3 and 4 and we expected that, as the temperature increases and the phonon gas distribution changes from 2D to 3D, x should change continuously from 3.5 to the value corresponding to 3D systems, which is 5.¹⁰ Instead of this, we observed that x does not have a monotonic behavior and totally disobeys the ansatz. It starts from $x = 3.5$ at low temperatures, it increases through the crossover region of temperatures around T_C and reaches a “plateau region” in which x varies in a small interval which lies between 4.5 and 5. The plateau region lies in a temperature range roughly between 0.5 and 5 K. After this, the exponent decreases steadily reaching values between 3.5 and 4 at the upper limit of the temperature range investigated by us, which is 10 K.

The results did not confirm the behavior of the heat power in the corresponding limits, as expected from the literature. Nevertheless, the exponent x should convey valuable information regarding the dispersion relations and the dimensionalities of the phonon system and of the electrons system. More analytical work is needed to clarify these connections.

ACKNOWLEDGMENTS

We are grateful to Dr. Sergiu Cojocaru for useful discussions and for his comments on the manuscript. This work was supported in part by the Romania-JINR

collaboration projects, positions 22, 23, 24, 27, Order 322/21.05.2018 (IFIN-HH), and position 24, Order 323/21.05.2018 (JINR). DVA was supported by the ANCS project PN18090101/2018.

-
- ¹ F. Giazotto, T. T. Heikkilä, A. Luukanen, A. M. Savin, and J. P. Pekola, *Rev. Mod. Phys.* **78**, 217 (2006).
- ² H. Q. Nguyen, M. Meschke, H. Courtois, and J. P. Pekola, *Phys. Rev. Appl.* **2**, 054001 (2014).
- ³ D. Anghel and S. Cojocaru, *Solid State Commun.* **227**, 56 (2016).
- ⁴ D. V. Anghel and S. Cojocaru, *Eur. Phys. J. B* **90**, 260 (2017).
- ⁵ D. V. Anghel, J. P. Pekola, M. M. Leivo, J. K. Suoknuuti, and M. Manninen, *Phys. Rev. Lett.* **81**, 2958 (1998).
- ⁶ D. V. Anghel and M. Manninen, *Phys. Rev. B* **59**, 9854 (1999).
- ⁷ T. Kühn, D. V. Anghel, J. P. Pekola, M. Manninen, and Y. M. Galperin, *Phys. Rev. B* **70**, 125425 (2004).
- ⁸ T. Kühn, D. V. Anghel, Y. M. Galperin, and M. Manninen, *Phys. Rev. B* **76**, 165425 (2007), cond-mat/07051936.
- ⁹ Note that we don't aim at *calculation* of the temperatures T_e and T_{ph} , which may differ from the temperature of bulk substrate (the thermostat). Therefore we do not need to include phonon-electron scattering explicitly.
- ¹⁰ F. C. Wellstood, C. Urbina, and J. Clarke, *Phys. Rev. B* **49**, 5942 (1994).
- ¹¹ J. K. Viljas and T. T. Heikkilä, *Phys. Rev. B* **81**, 245404 (2010).
- ¹² S. Cojocaru and D. V. Anghel, *Phys. Rev. B* **93**, 115405 (2016).
- ¹³ F. W. J. Hekking, A. O. Niskanen, and J. P. Pekola, *Phys. Rev. B* **77**, 033401 (2008).
- ¹⁴ D. V. Anghel and L. Kuzmin, *Appl. Phys. Lett.* **82**, 293 (2003).
- ¹⁵ D. V. Anghel, A. Luukanen, and J. P. Pekola, *Appl. Phys. Lett.* **78**, 556 (2001).
- ¹⁶ B. A. Auld, *Acoustic Fields and Waves in Solids, 2nd Ed.* (Robert E. Krieger Publishing Company, 1990).
- ¹⁷ D. V. Anghel and T. Kühn, *J. Phys. A: Math. Theor.* **40**, 10429 (2007), cond-mat/0611528.
- ¹⁸ Ziman, *Electrons and Phonons* (Harcourt College Publishers, 1976).